Electronic Supplementary Material (ESI) for ChemComm.

$[Ru(phen)_2dppz]^{2+}$ Luminescence Reveals Nanoscale Variation of Polarity in the Cyclodextrin Cavity

Patrick Higgs,[a] Andrew W. McKinley,[b] and Eimer M. Tuite[a]*

a. Chemical Nanoscience Laboratory, School of Chemistry, Newcastle University, Newcastle upon Tyne, NE1 7RU, UK.

b: Department of Chemistry, Imperial College London, London SW7 2AZ, UK.

E-mail: a.mckinley@imperial.ac.uk

* Corresponding author. Fax: +44 (0)191 2226929; Tel: +44 (0)191 2225523; E-mail: eimer.tuite@ncl.ac.uk

Supporting Information

MATERIALS AND METHODS

The Δ– and Λ–enantiomers of $[Ru(phen)_2dppz]Cl_2$, $[Ru(bpy)_2dppz]Cl_2$, $[Ru(bpy)_3]Cl_2$, and $[Ru(phen)_3]Cl_2$ were prepared and purified as previously described [C. Hiort, P. Lincoln, B. Nordén, J. Am. Chem. Soc. 115 (1993) 3448-3454; P. Lincoln, B. Nordén, J. Phys. Chem. B 102 (1998) 9583-9594]. Luminescence excitation spectroscopy was used to establish that emissive impurities made no contribution above baseline emission. Enantiomeric purity was established by CD spectroscopy (Jasco J-720). The concentrations of ruthenium complexes were determined using the following extinction coefficients in water: $[Ru(phen)_2dppz]^{2+}$, ε(439 nm) = 20,000 M^{-1} cm^{-1}; $[Ru(bpy)_2dppz]^{2+}$, ε(444 nm) = 16,100 M^{-1} cm^{-1}; $[Ru(phen)_3]^{2+}$, ε(445 nm) = 19,000 M^{-1} cm^{-1}; $[Ru(bpy)_3]^{2+}$, ε(452 nm) = 14,600 M^{-1} cm^{-1}.

β-cyclodextrin hydrate (Sigma, 99%) and β-cyclodextrin phosphate sodium salt (Sigma, ≥95%, 2-6 mol phosphate per mol cyclodextrin) and γ-cyclodextrin (Sigma, ≥98%) were used as received. Concentrations were determined by mass, and the average β-cyclodextrin phosphate sodium salt molar mass was calculated with 4 mol phosphate per mol cyclodextrin.

All experiments were carried out in ultrapure water. Absorption spectra were recorded with a Cary 100-Bio UV/vis spectrometer. Emission and excitation spectra were recorded on a SPEX Fluoromax spectrofluorimeter. Emission lifetimes were measured by single-photon counting with excitation at 405 nm and emission at 625 nm.

Binding constants at low $[\beta\text{-}P_nCD]/[Ru]$ ratios were estimated using the Benesi-Hildbrand method, assuming 1:1 stoichiometry using Equation (1) for absorbance and Equation (2) for emission [H.A. Benesi, J.H. Hildebrand, J. Am. Chem. Soc. 71 (1949) 2703-2707].

$$\frac{1}{A - A_0} = \frac{1}{K(A_\infty - A_0)} \bullet \frac{1}{[CD]_0} + \frac{1}{(A_\infty - A_0)} \qquad (1)$$

$$\frac{1}{F - F_0} = \frac{1}{K(F_\infty - F_0)} \bullet \frac{1}{[CD]_0} + \frac{1}{(F_\infty - F_0)} \qquad (2)$$

where A is absorbance, F is emission intensity, and K is the equilibrium constant for association of the ruthenium complex with $\beta\text{-}P_nCD$. When $1/(A–A_0)$ or $1/(F–F_0)$ is plotted against $1/[CD]_0$, the binding constant equates to y-intercept/gradient.

Stern-Volmer analysis was applied to emission data to determine rate constants for quenching of the ruthenium complexes by oxygen using Equation (3).

$$\frac{F_0}{F} = 1 + k_q \tau_0 [Q] \qquad (3)$$

where τ_0 is the lifetime in the absence of quencher. The concentrations of oxygen in water are 0.3 mM in air and 0.0 mM under inert gas ["Handbook of Photochemistry" M. Montalti, A. Credi, L. Prodi, M. T. Gandolfi, 3rd Edn. (Taylor & Francis) 2006.]. These values were used both in the absence and presence of $\beta\text{-}P_nCD$.

ADDITIONAL EXPERIMENTAL DATA

Table S1. Emission lifetimes and emission spectral maxima of Δ-$[Ru(phen)_2dppz]^{2+}$ in air at 293-298 K.

solvent	**λ_{max} / nm**	**τ / ns (air)**	**τ / ns (Ar)**
dimethylformamide [1]	663	181	255
acetonitrile [1]	634	174	213
ethanol [1]	619	153	175
1,2-propanediol [2]	620	-	86
methanol [1]	627	27	29
1,3-propanediol [2]	620	-	27
formamide [1]	660	13	12
glycerol [2]	639	-	8.2
ethylene glycol [2]	656	-	7.5
water [3]	800	-	0.8
polymer		**-**	
poly(dA) [4]	650	5/67/216	-
poly(dT) [4]	647	7/84/248	-

[1] A.W. McKinley, PhD Thesis, University of Newcastle upon Tyne, 2008. *Photophysics of Light Switch Ruthenium Complexes and Their Interactions with DNA*.

[2] J. Olofsson, L.M. Wilhelmsson, P. Lincoln, *J. Am. Chem. Soc.* 126 (2004) 15458-15465.

[3] E.J.C. Olson, D. Hu, A. Hormann, A.M. Jonkman, M.R. Arkin, E.D.A. Stemp, J.K. Barton, P.F. Barbara, *J. Am. Chem. Soc.* 119 (1997) 11458-11467.

[4] J.M. Moon, J.-M. Lee, J.Y. Choi, H.M. Lee, S.K. Kim, *J. Inorg. Biochem.* 101 (2007) 1386-1393.

Table S2. Equilibrium constants for initial interaction with β-P_nCD using Benesi-Hildebrand method, assuming formation of a 1:1 complex.

	Λ-$[Ru(phen)_2dppz]^{2+}$	**Δ-$[Ru(phen)_2dppz]^{2+}$**	**Δ-$[Ru(bpy)_2dppz]^{2+}$**	**Δ-$[Ru(phen)_3]^{2+}$**	**Δ-$[Ru(bpy)_3]^{2+}$**
abs	3.37×10^3	1.01×10^5	5.09×10^4	5.51×10^5	6.75×10^5
em	4.75×10^3	2.03×10^4	1.66×10^4	1.19×10^4	1.07×10^5
av	**4.06×10^3**	**6.07×10^4**	**3.38×10^4**	**2.81×10^5**	**3.91×10^5**
log(*K*)	**3.61**	**4.78**	**4.53**	**5.45**	**5.59**

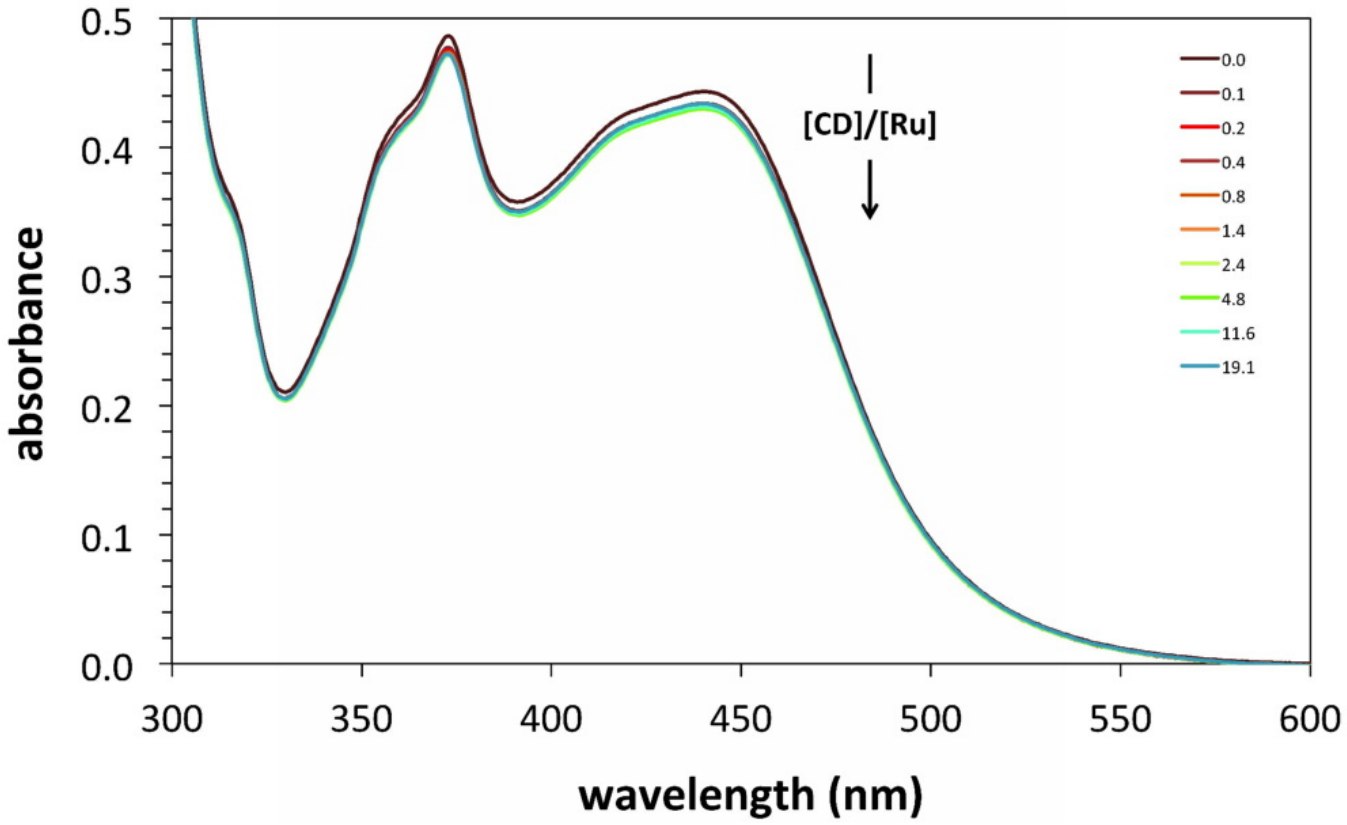

Figure S1. Absorption spectra of Δ-$[Ru(phen)_2dppz]^{2+}$ with added β-CD. [Ru] = 20 μM. Legend shows [β-CD]/[Ru] ratios.

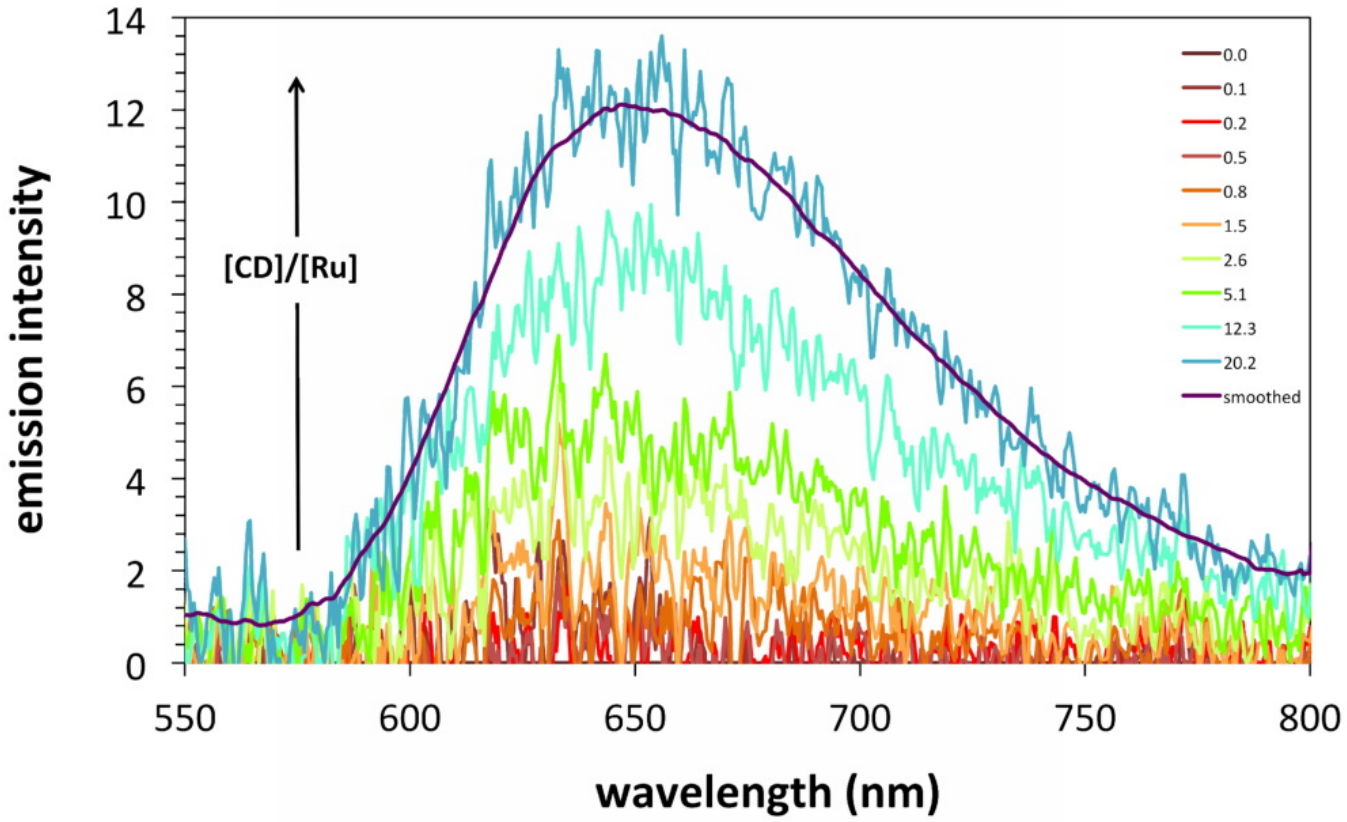

Figure S2. Emission spectra of Δ-$[Ru(phen)_2dppz]^{2+}$ with added β-CD. λ_{ex} = 410 nm. [Ru] = 20 μM. Legend shows [β-CD]/[Ru] ratios.

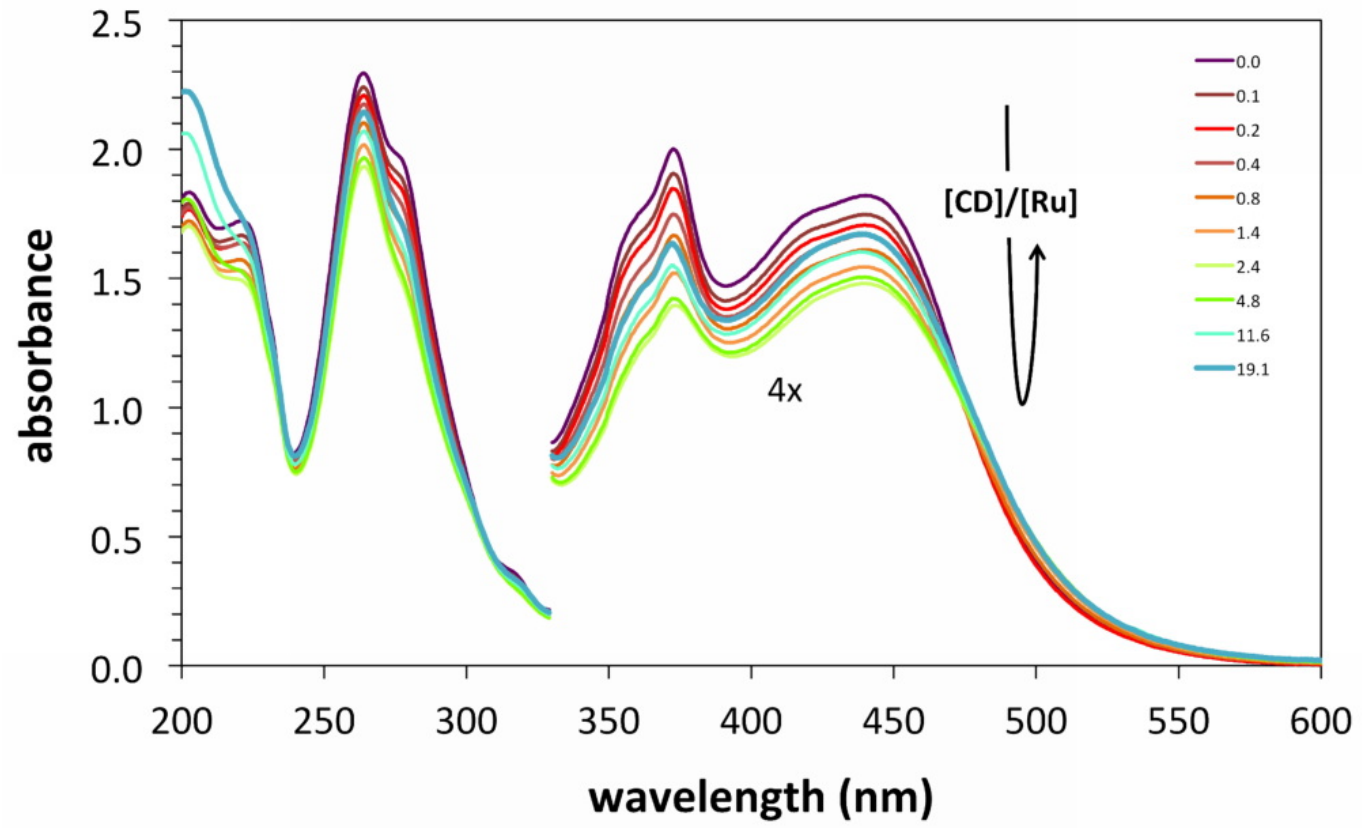

Figure S3. Absorption spectra of Δ-[Ru(phen)$_2$dppz]$^{2+}$ with added β-CD-phosphate. [Ru] = 20 μM. Legend shows [β-P$_n$CD]/[Ru] ratios.

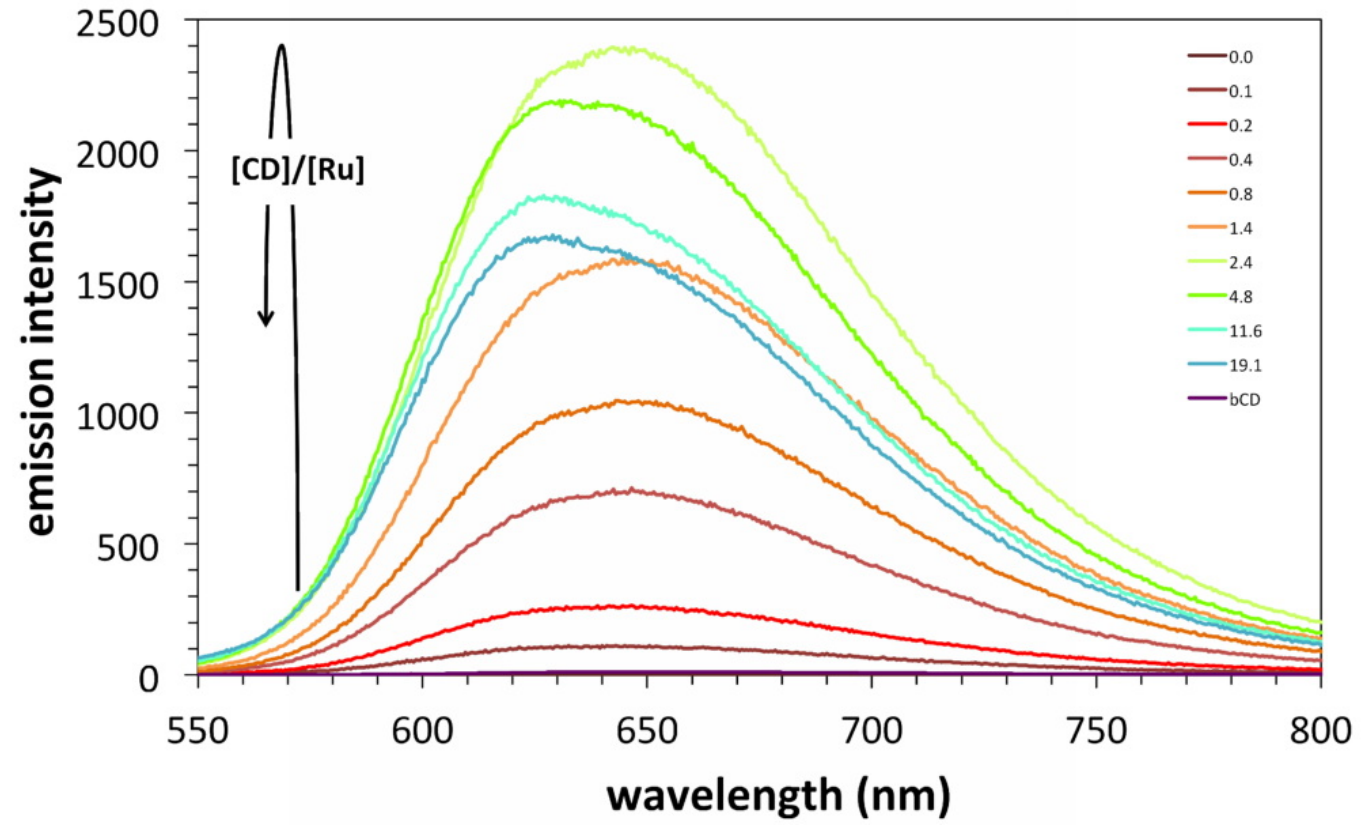

Figure S4. Emission spectra of Δ-[Ru(phen)$_2$dppz]$^{2+}$ with added β-P$_n$CD. λ_{ex} = 475 nm. [Ru] = 20 μM. Legend shows [β-P$_n$CD]/[Ru] ratios. The spectrum with β-CD at a ratio of 20 is shown for comparison.

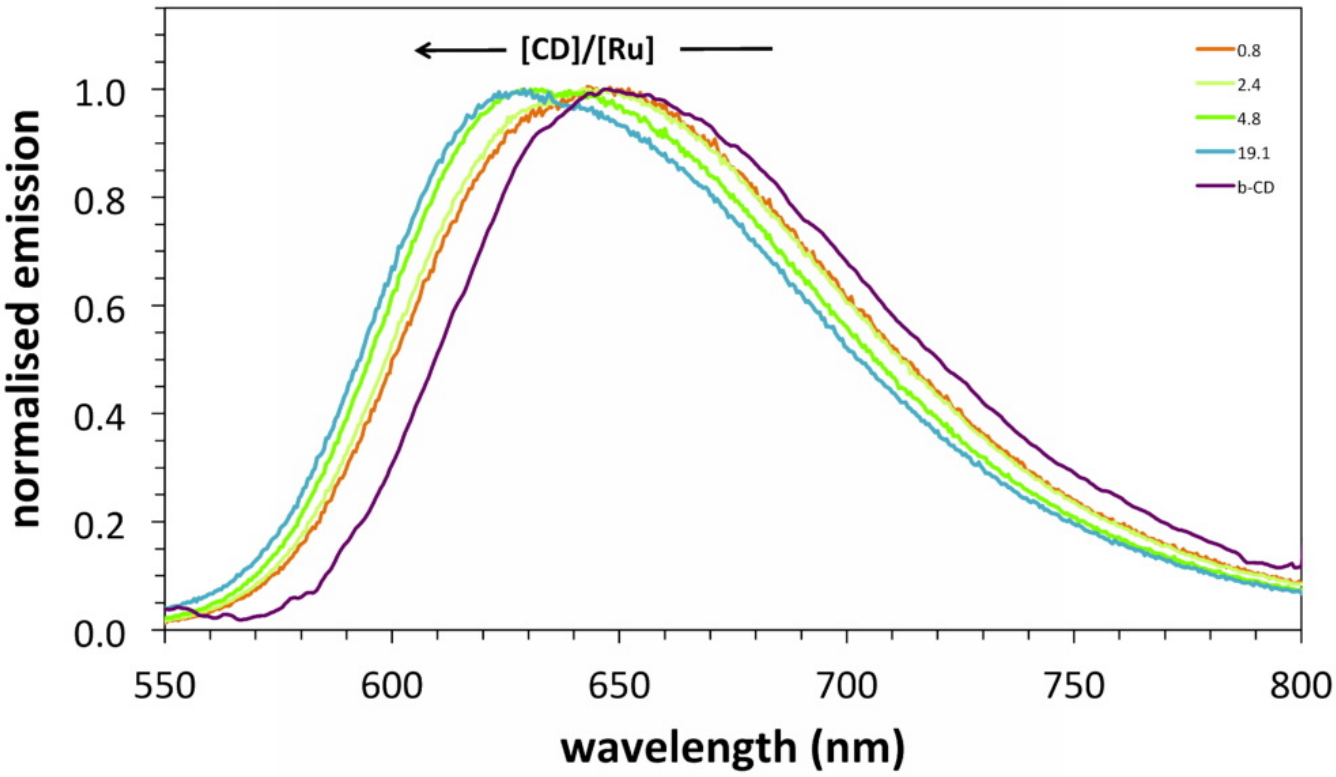

Figure S5. Normalised emission spectra of Δ-[Ru(phen)$_2$dppz]$^{2+}$ with added β-P$_n$CD. λ_{ex} = 475 nm. [Ru] = 20 μM. Legend shows [β-P$_n$CD]/[Ru] ratios. The spectrum with β-CD at a ratio of 20 is shown for comparison.

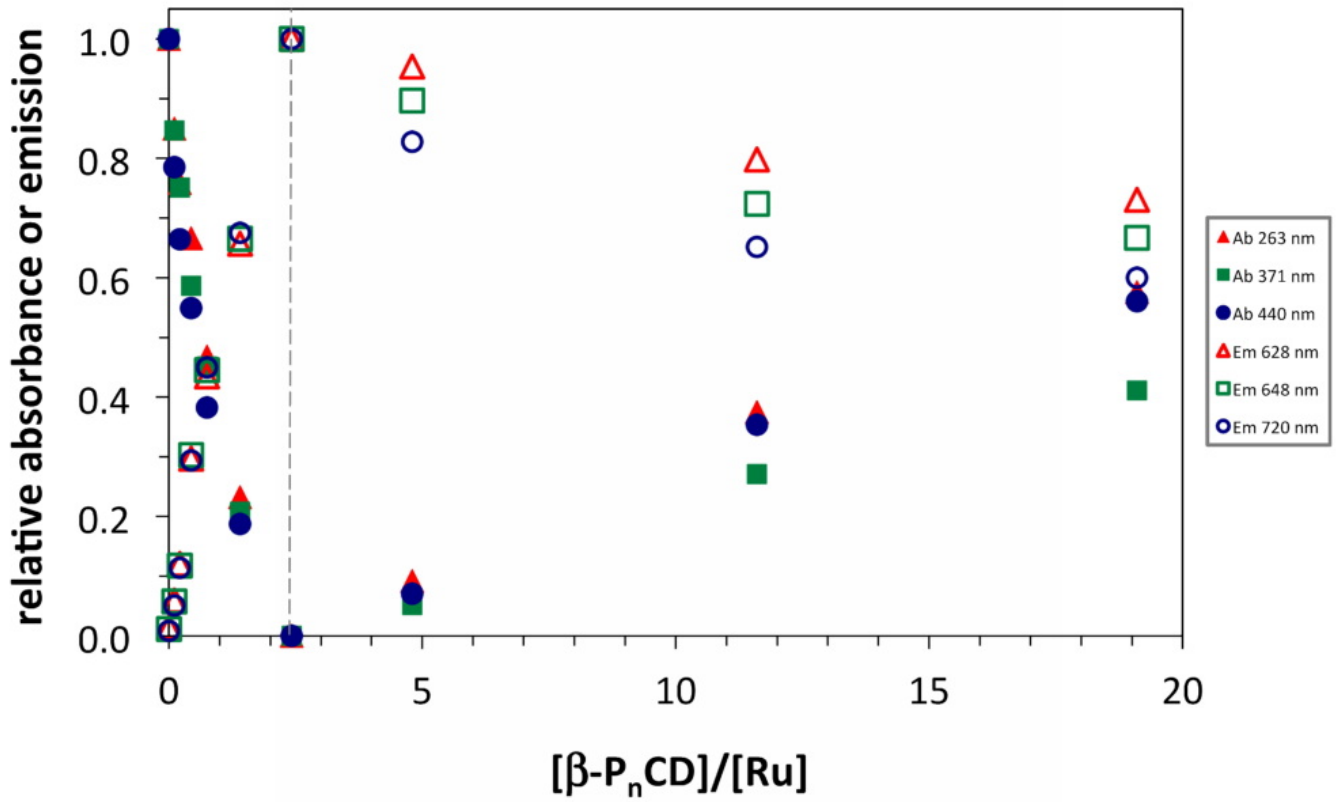

Figure S6. Normalized absorption and emission changes of Δ-[Ru(phen)$_2$dppz]$^{2+}$ as a function of added β-P$_n$CD. [Ru] = 20 μM. The legend shows the monitored wavelengths.

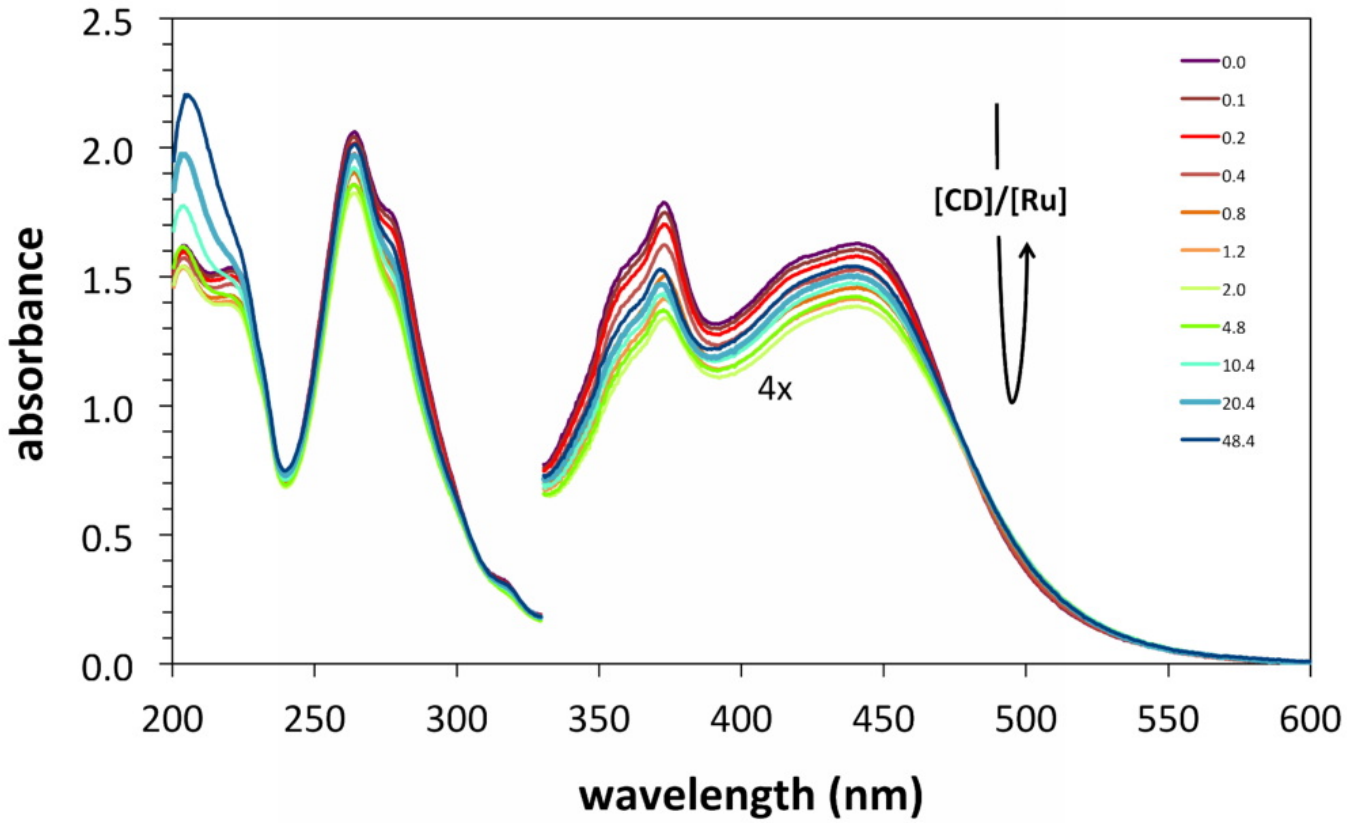

Figure S7. Absorption spectra of Λ-$[Ru(phen)_2dppz]^{2+}$ with added β-CD-phosphate. [Ru] = 20 μM. Legend shows [β-P_nCD]/[Ru] ratios.

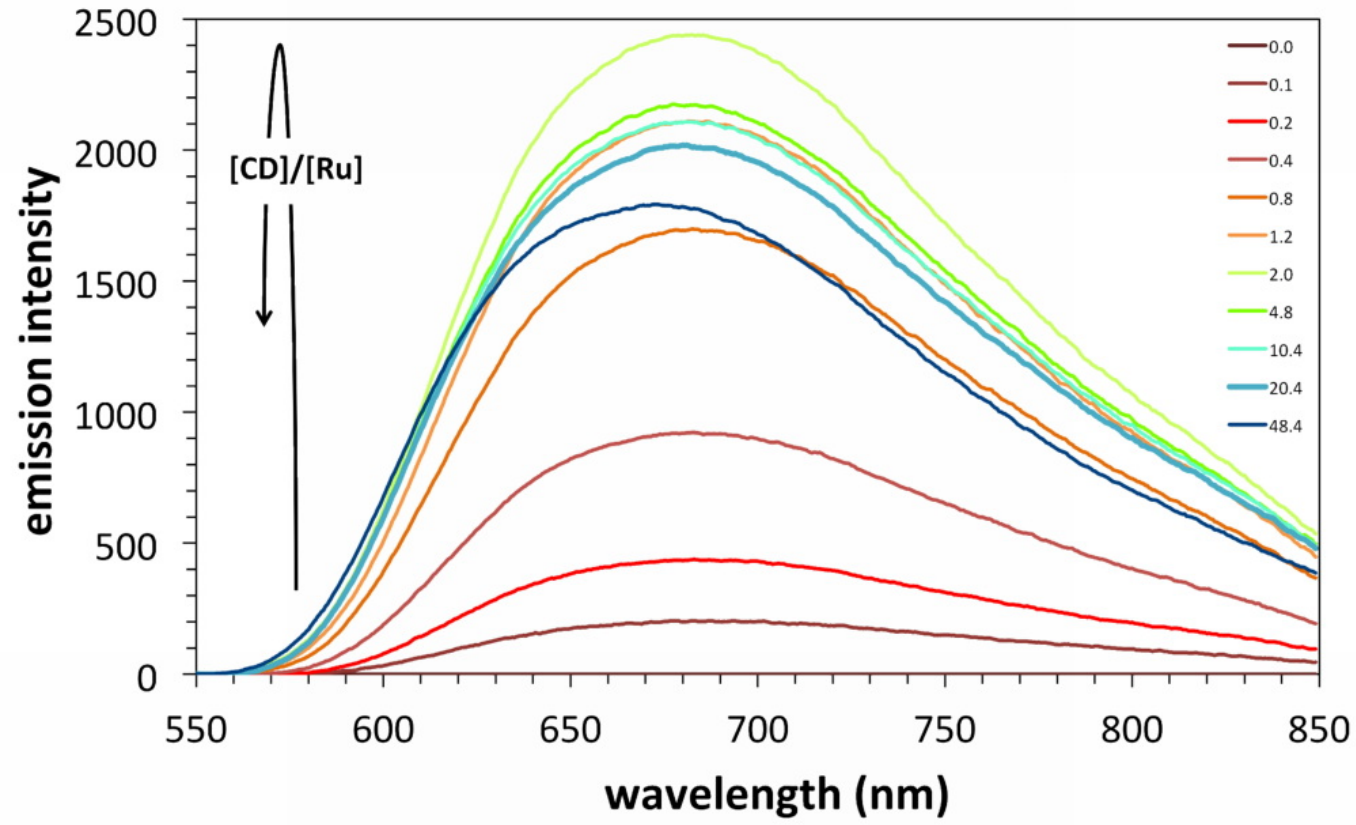

Figure S8. Emission spectra of Λ-$[Ru(phen)_2dppz]^{2+}$ with added β-P_nCD. λ_{ex} = 475 nm. [Ru] = 20 μM. Legend shows [β-P_nCD]/[Ru] ratios.

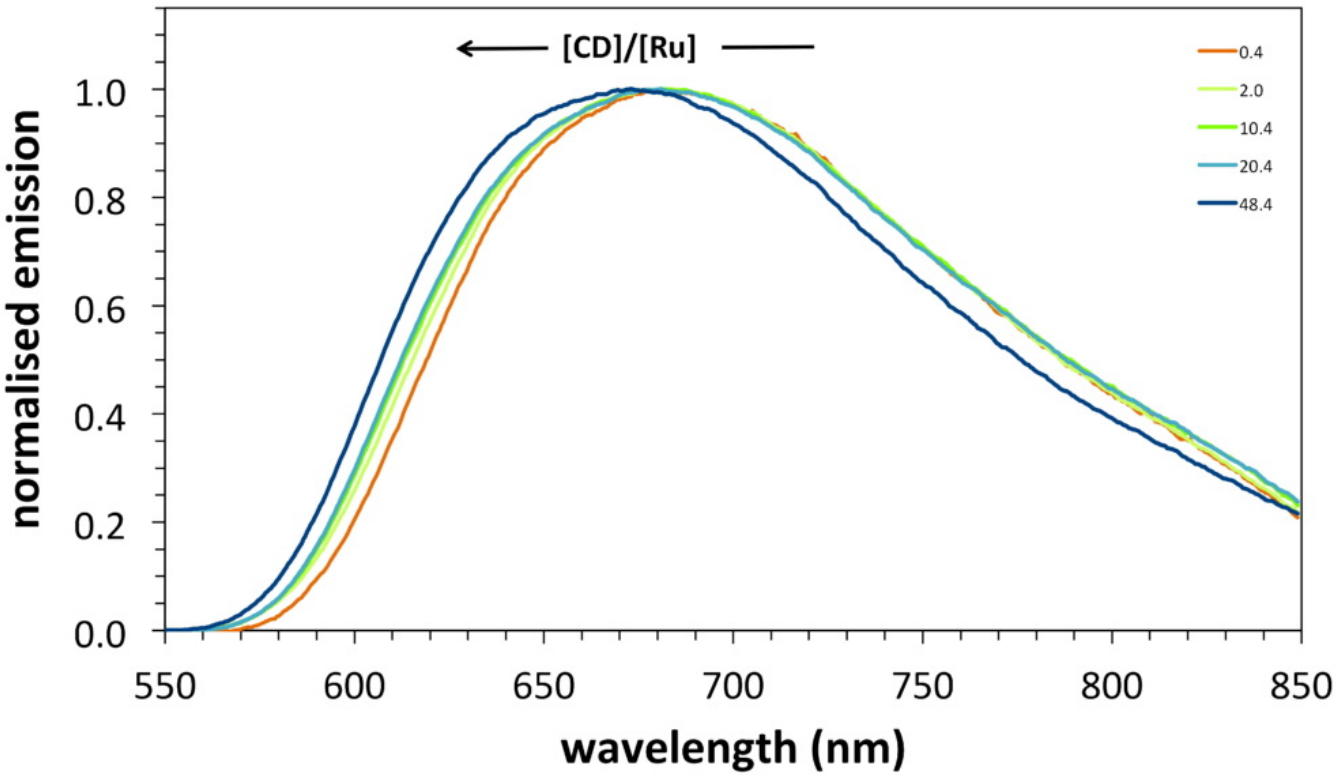

Figure S9. Normalised emission spectra of Λ-[Ru(phen)$_2$dppz]$^{2+}$ with added β-P$_n$CD. λ_{ex} = 475 nm. [Ru] = 20 μM. Legend shows [β-P$_n$CD]/[Ru] ratios.

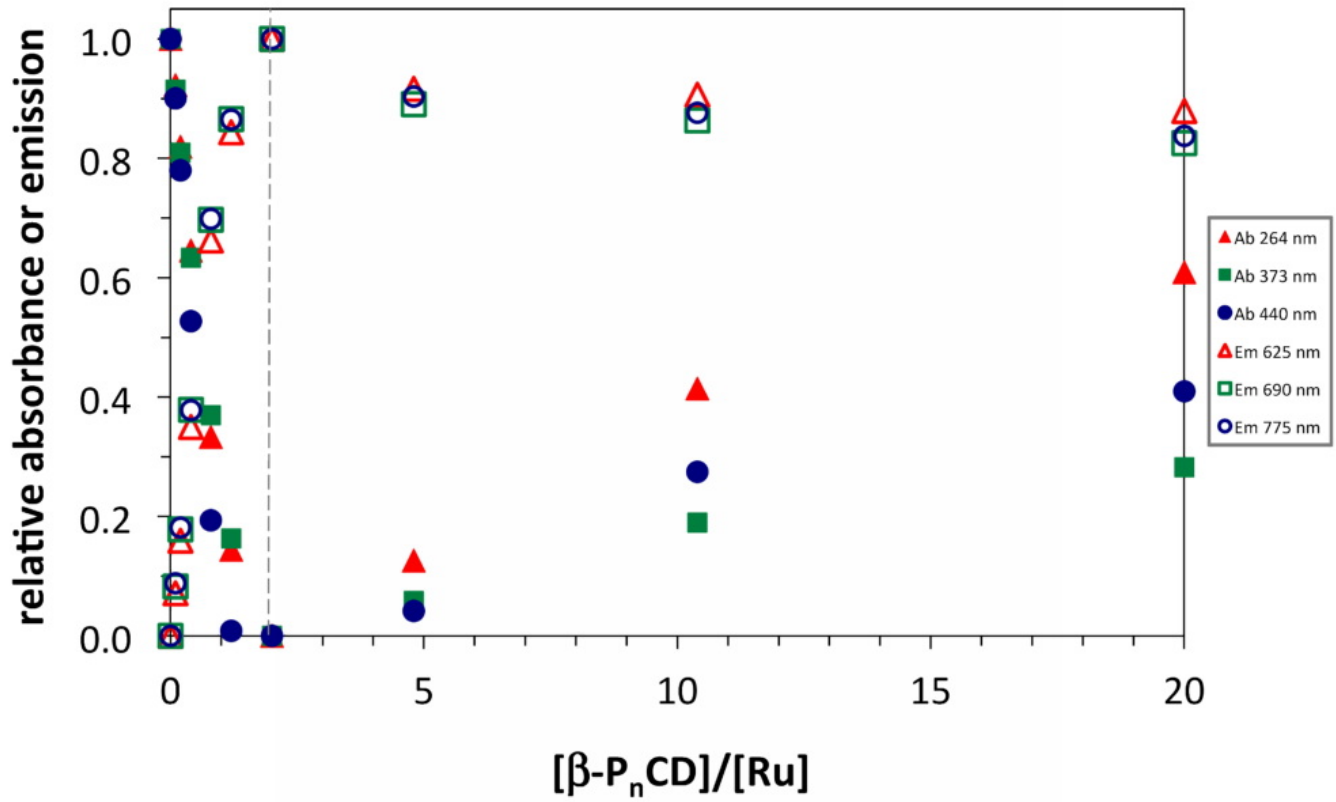

Figure S10. Normalized absorption and emission changes of Λ-[Ru(phen)$_2$dppz]$^{2+}$ as a function of added β-P$_n$CD. [Ru] = 20 μM. The legend shows the monitored wavelengths.

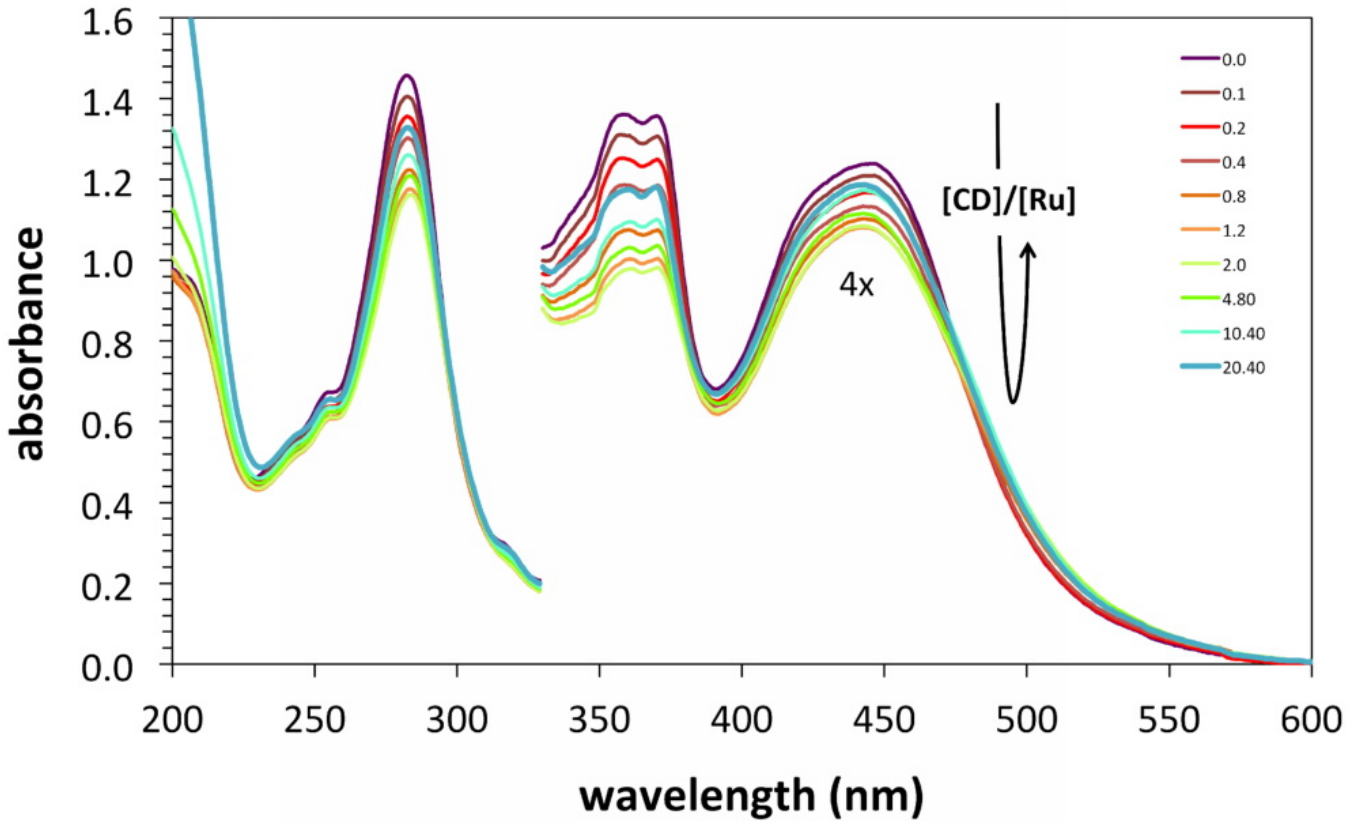

Figure S11. Absorption spectra of Δ-$[Ru(bpy)_2dppz]^{2+}$ with added β-CD-phosphate. [Ru] = 20 μM. Legend shows [β-P_nCD]/[Ru] ratios.

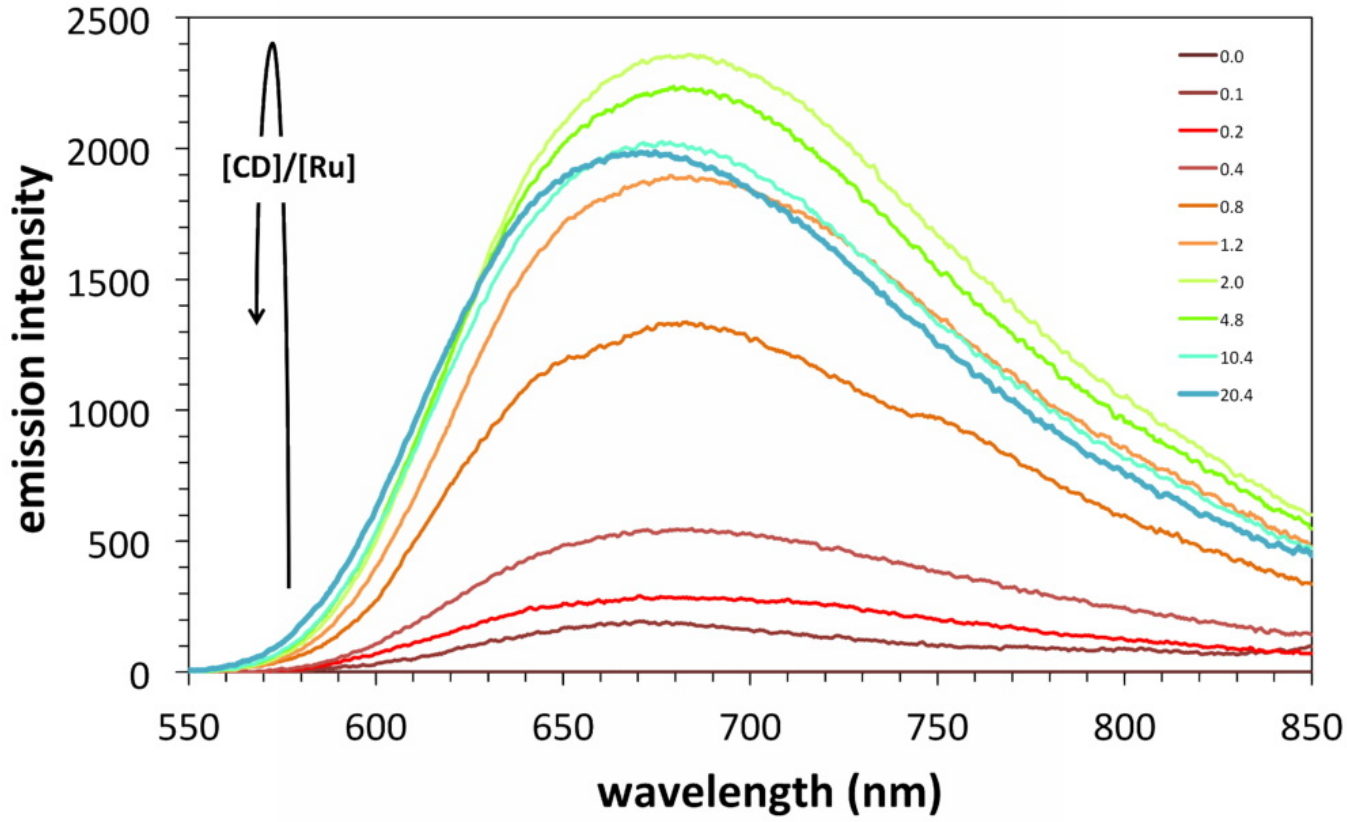

Figure S12. Emission spectra of Δ-$[Ru(bpy)_2dppz]^{2+}$ with added β-P_nCD. λ_{ex} = 470 nm. [Ru] = 20 μM. Legend shows [β-P_nCD]/[Ru] ratios.

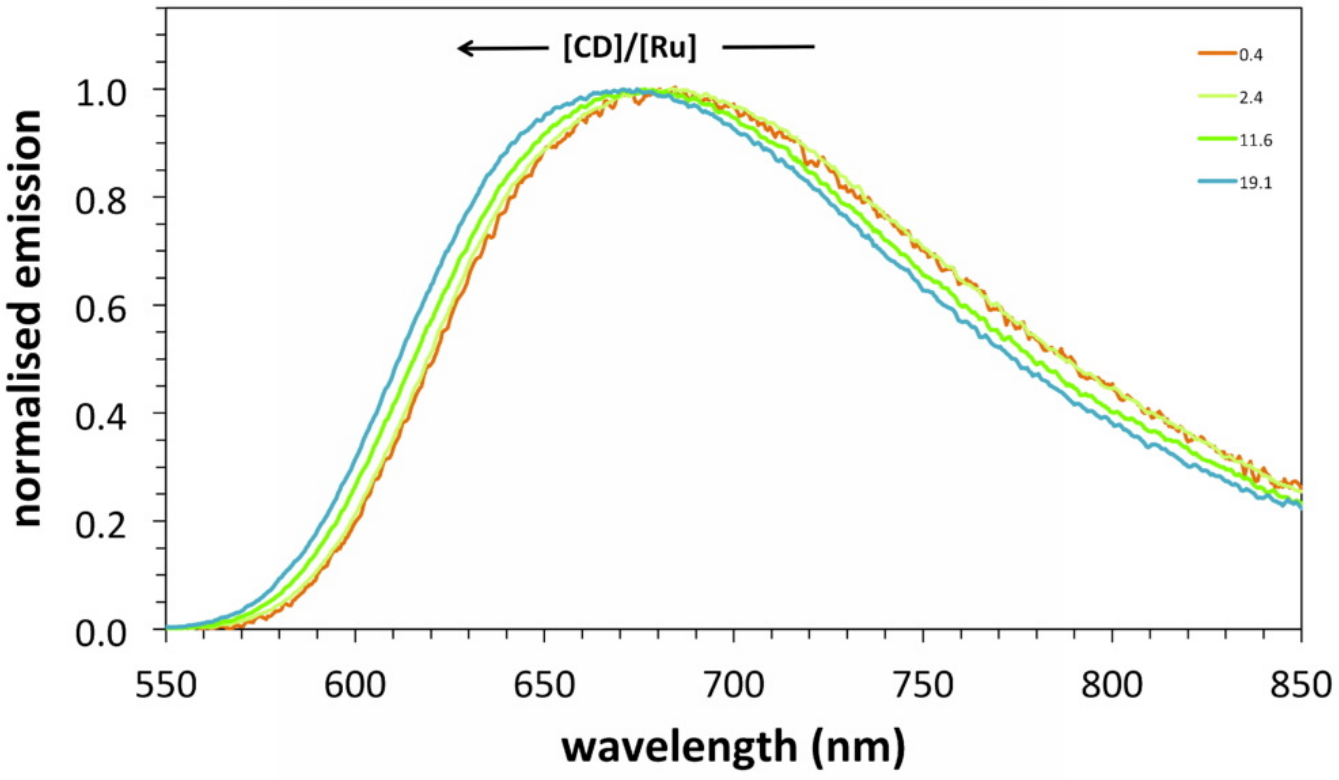

Figure S13. Normalised emission spectra of Δ-$[Ru(bpy)_2dppz]^{2+}$ with added β-P_nCD. λ_{ex} = 470 nm. [Ru] = 20 μM. Legend shows [β-P_nCD]/[Ru] ratios.

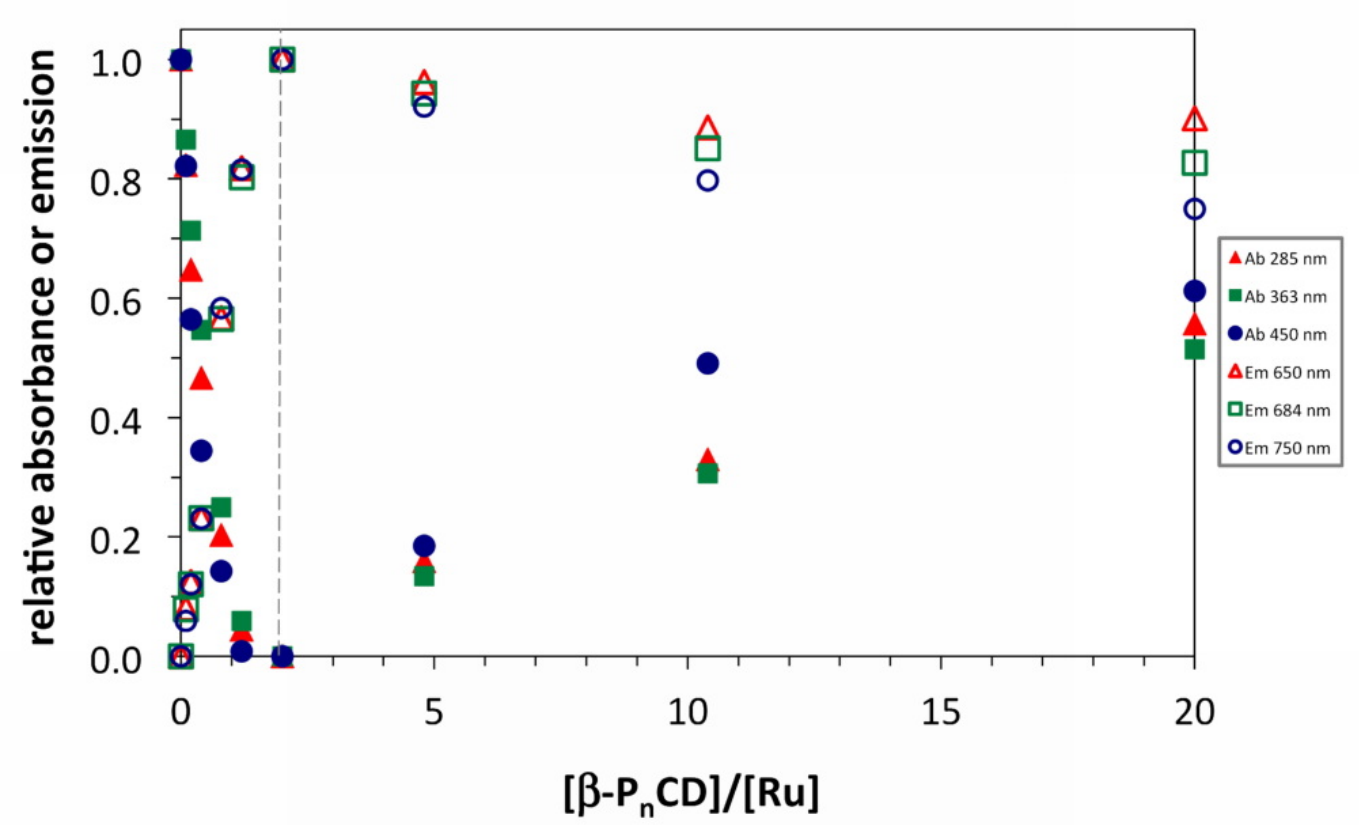

Figure S14. Normalized absorption and emission changes of Δ-$[Ru(bpy)_2dppz]^{2+}$ as a function of added β-P_nCD. [Ru] = 20 μM. The legend shows the monitored wavelengths.

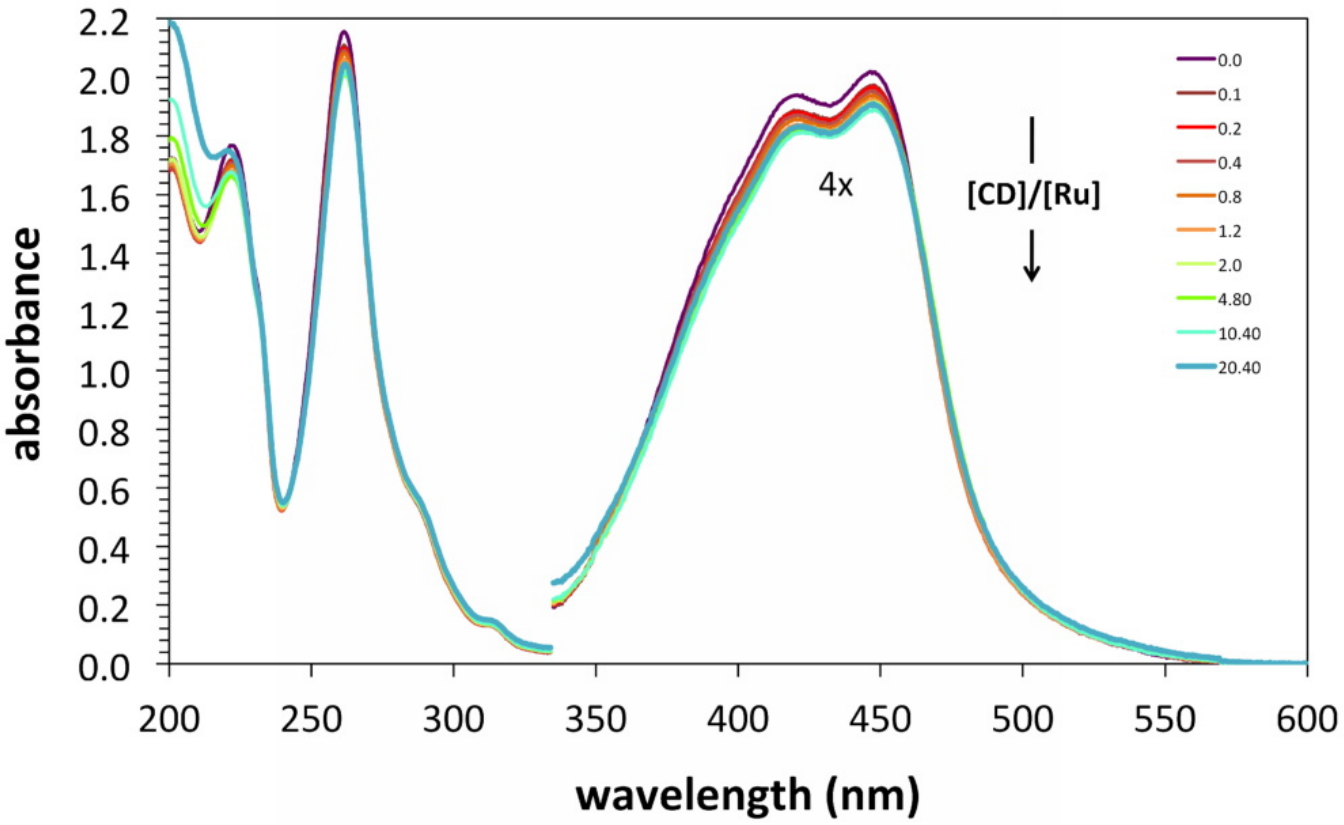

Figure S15. Absorption spectra of Δ-$[Ru(phen)_3]^{2+}$ with added β-CD-phosphate. [Ru] = 20 μM. Legend shows [β-P_nCD]/[Ru] ratios.

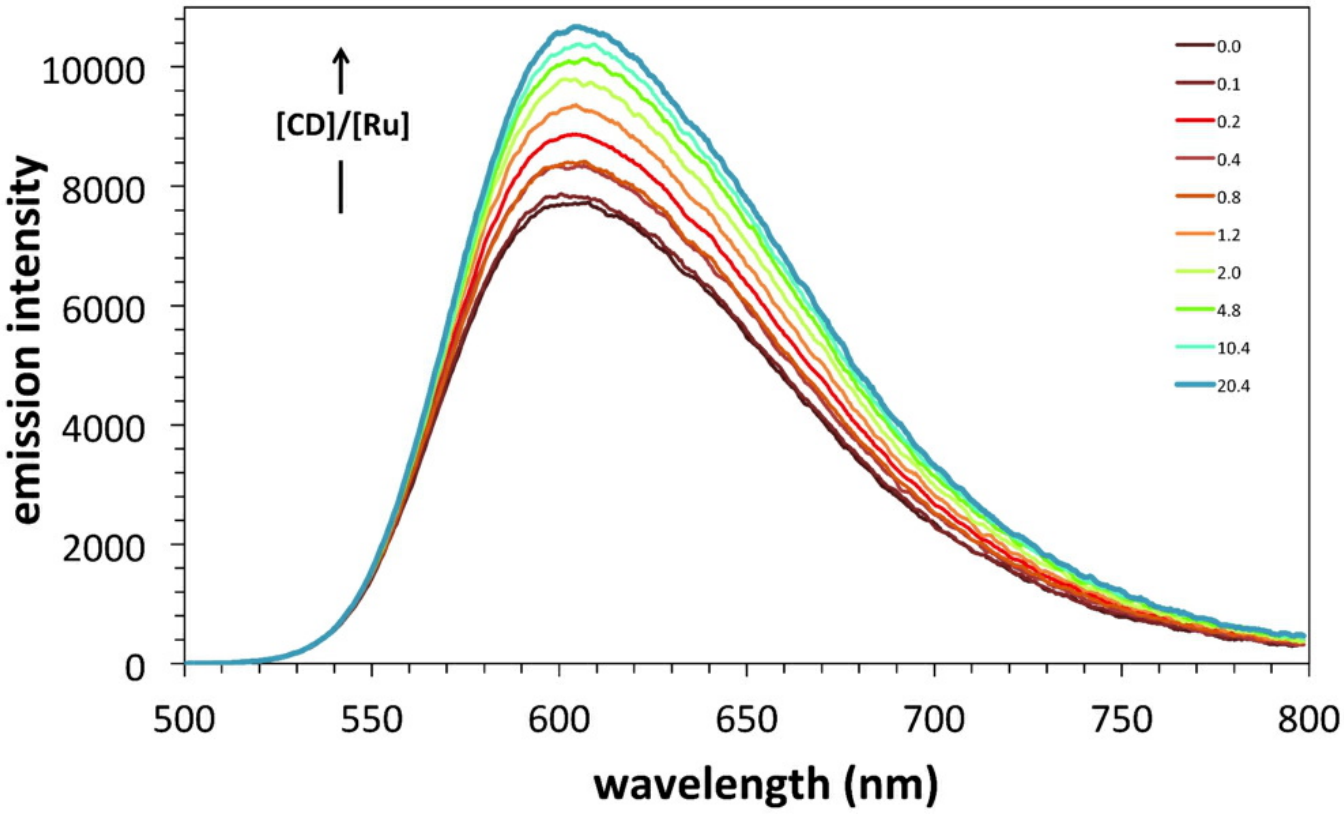

Figure S16. Emission spectra of Δ-$[Ru(phen)_3]^{2+}$ with added β-P_nCD. λ_{ex} = 470 nm. [Ru] = 20 μM. Legend shows [β-P_nCD]/[Ru] ratios.

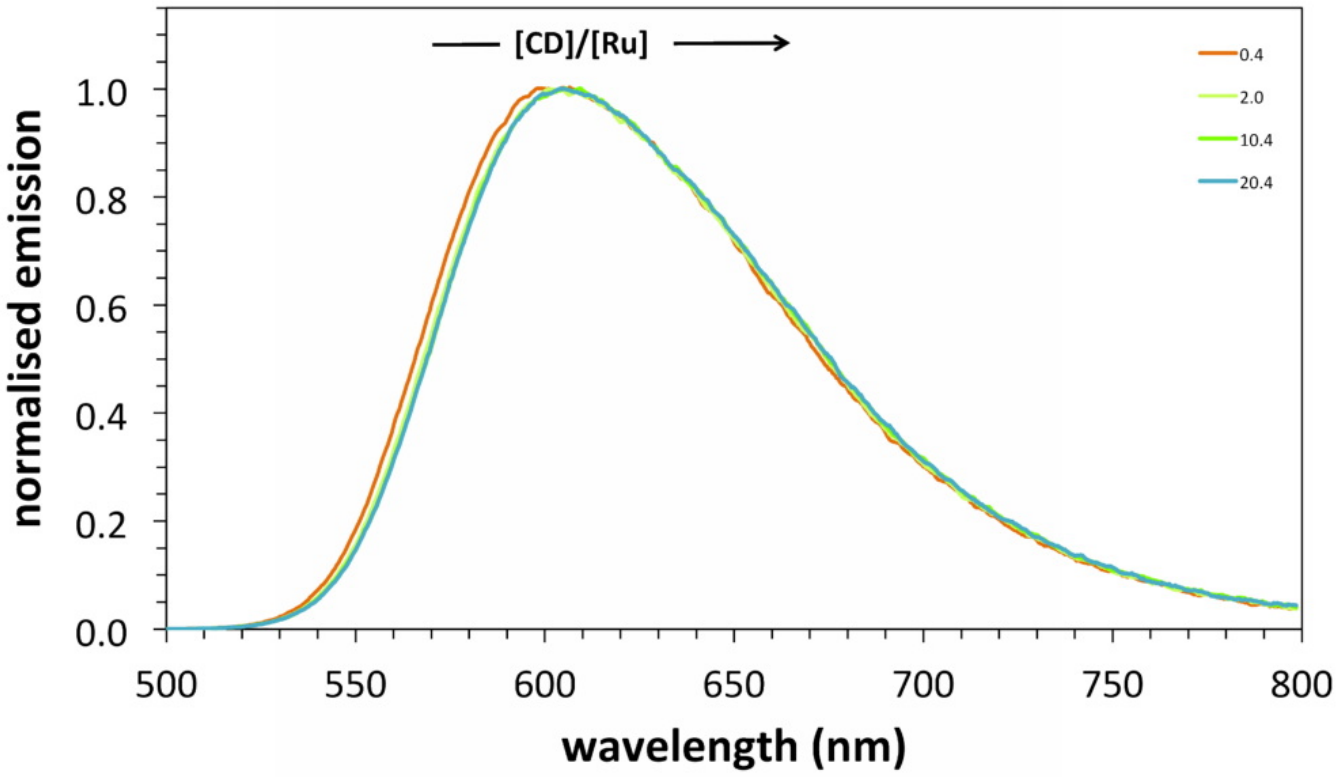

Figure S17. Normalised emission spectra of Δ-$[Ru(phen)_3]^{2+}$ with added β-P_nCD. λ_{ex} = 470 nm. [Ru] = 20 μM. Legend shows [β-P_nCD]/[Ru] ratios.

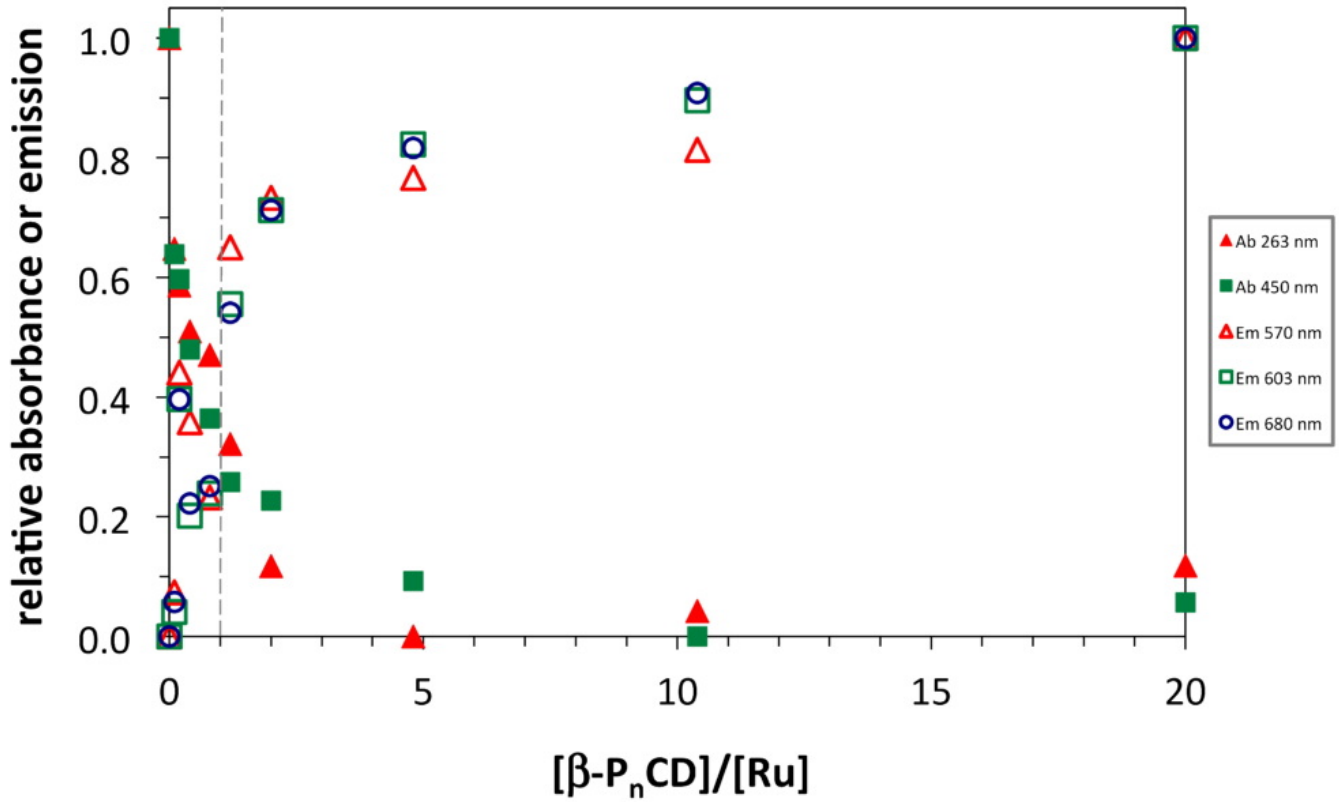

Figure S18. Normalized absorption and emission changes of Δ-$[Ru(phen)_3]^{2+}$ as a function of added β-P_nCD. [Ru] = 20 μM. The legend shows the monitored wavelengths.

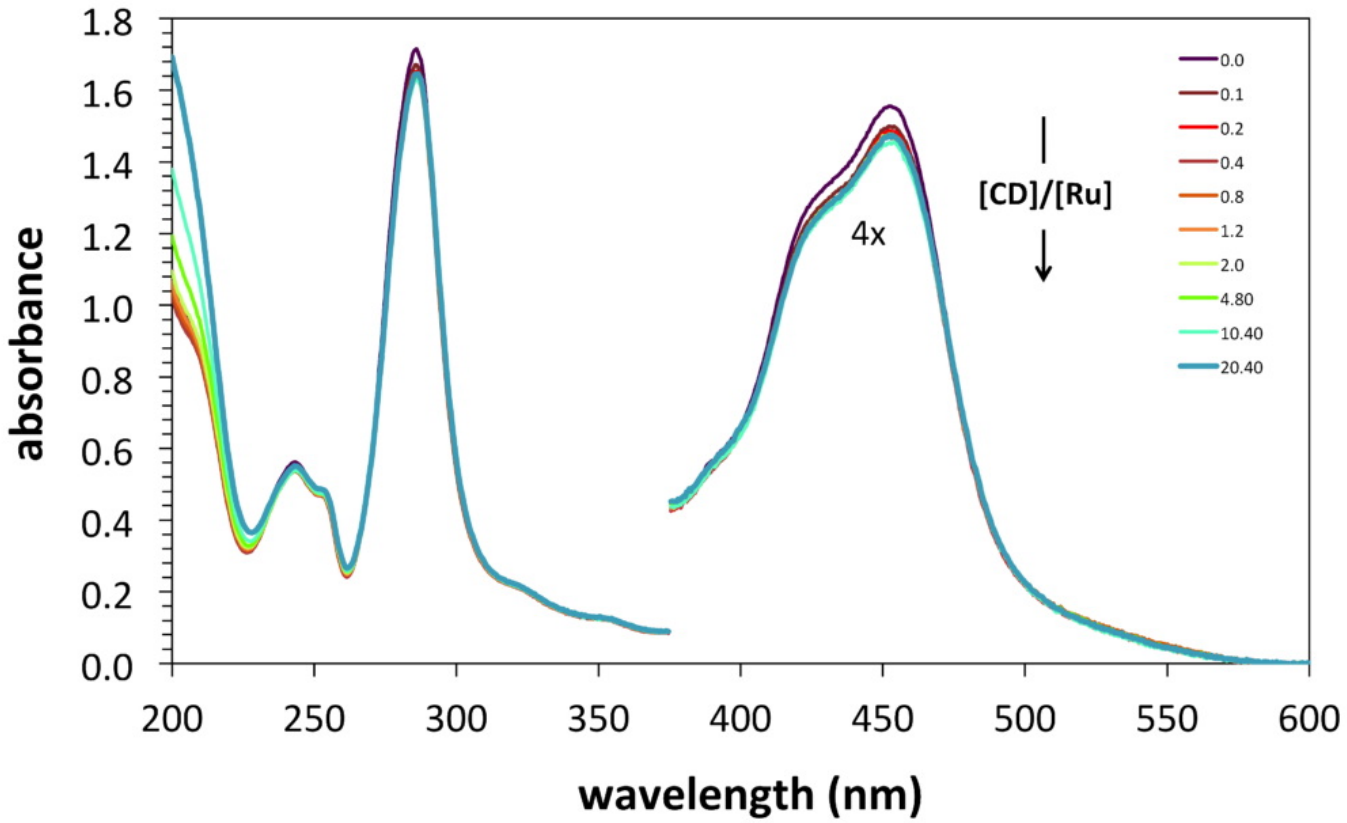

Figure S19. Absorption spectra of Δ-$[Ru(bpy)_3]^{2+}$ with added β-CD-phosphate. [Ru] = 20 μM. Legend shows [β-P_nCD]/[Ru] ratios.

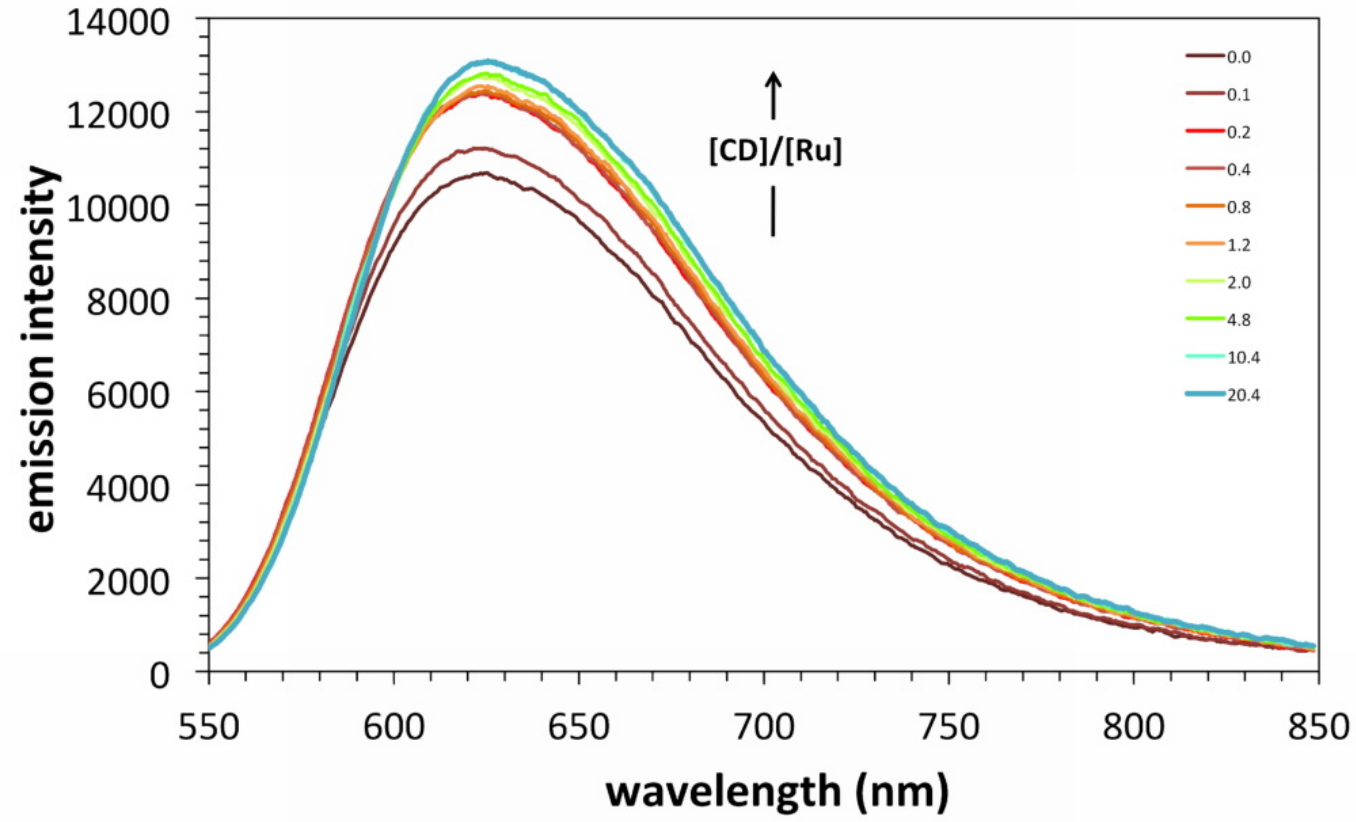

Figure S20. Emission spectra of Δ-$[Ru(bpy)_3]^{2+}$ with added β-CD-phosphate. λ_{ex} = 470 nm. [Ru] = 20 μM. Legend shows [β-P_nCD]/[Ru] ratios.

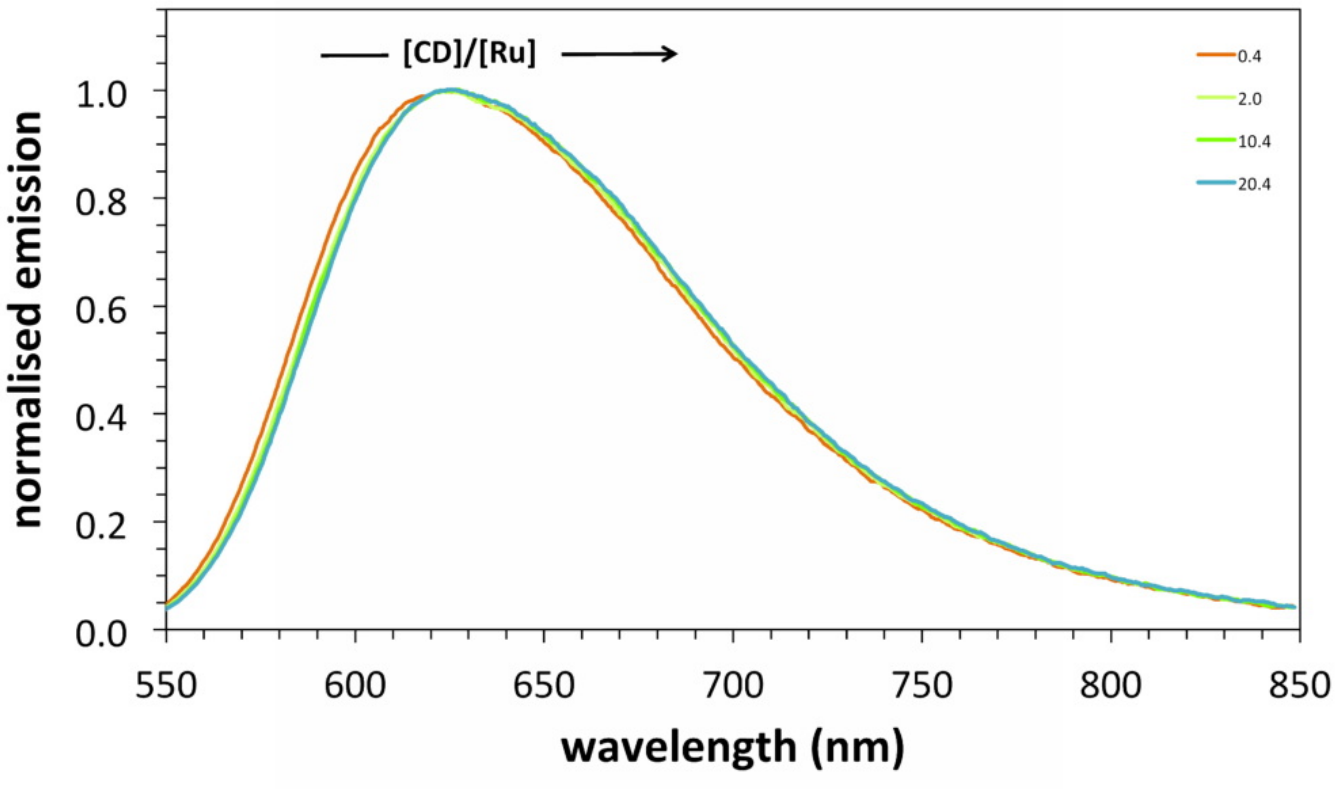

Figure S21. Normalised emission spectra of Δ-$[Ru(bpy)_3]^{2+}$ with added β-CD-phosphate. λ_{ex} = 470 nm. [Ru] = 20 μM. Legend shows [β-P_nCD]/[Ru] ratios.

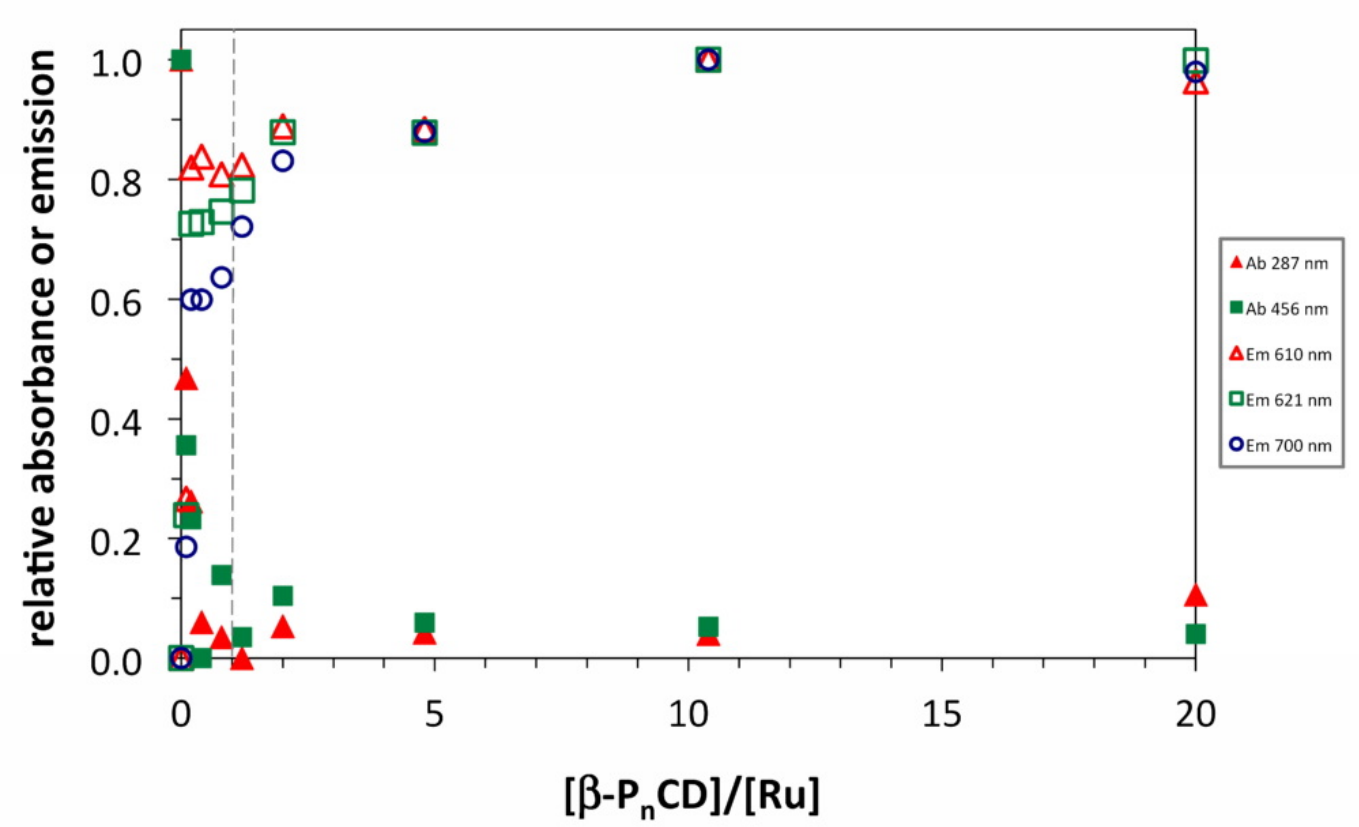

Figure S22. Relative intensities of Δ-$[Ru(bpy)_3]^{2+}$ with added β-CD-phosphate. [Ru] = 20 μM. Legend shows [β-P_nCD]/[Ru] ratios.

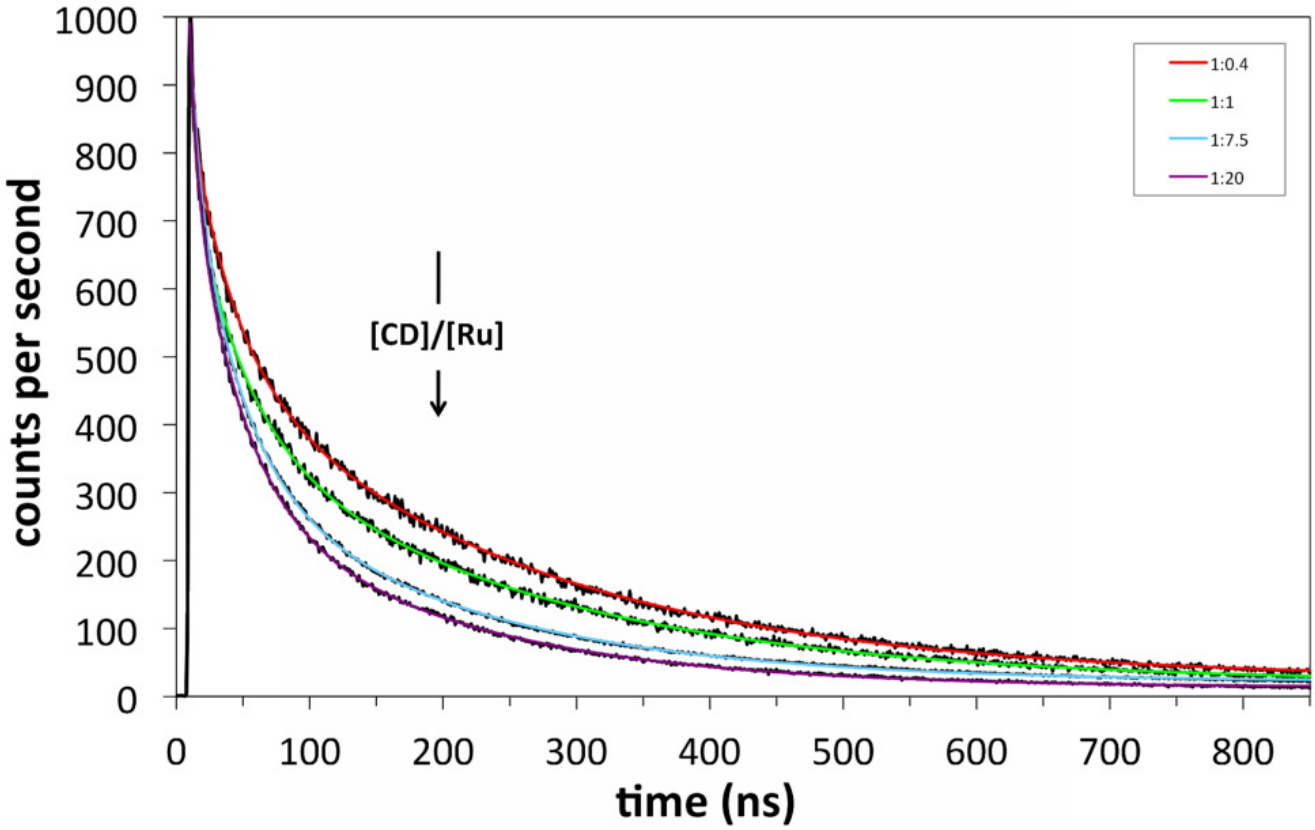

Figure S23. Single photon counting decays for Δ-$[Ru(phen)_2dppz]^{2+}$ with added β-CD-phosphate, with tri-exponential fits overlaid. λ_{ex} = 405 nm/ λ_{em} = 625 nm. [Ru] = 20 μM. Legend shows [β-P_nCD]/[Ru] ratios.

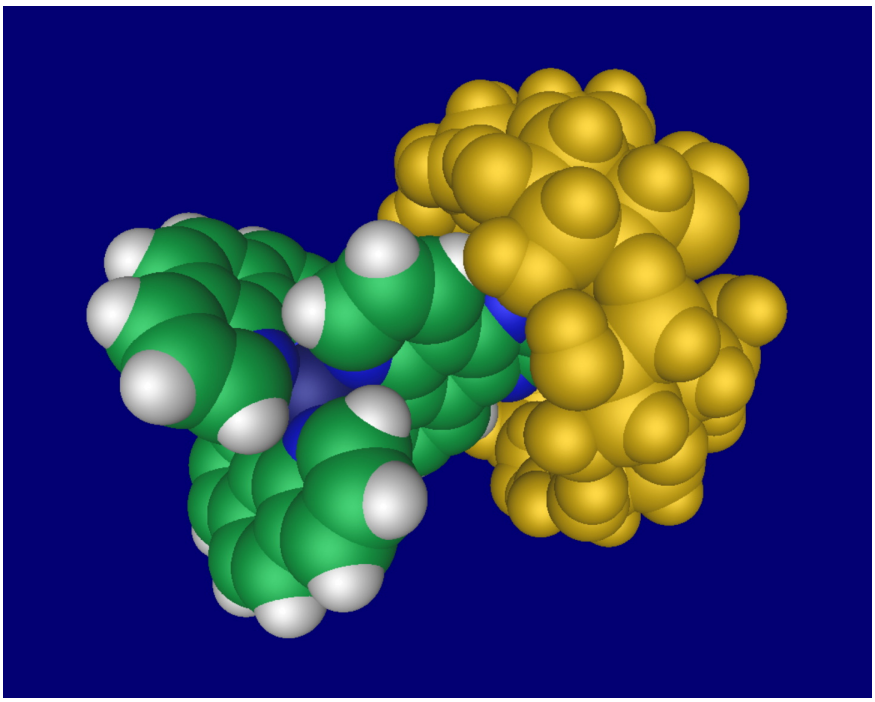

Figure S24. Model of the 1:1 docking complex formed between Δ-$[Ru(phen)_2dppz]^{2+}$ and β-CD. The metal complex geometry was minimized using the SPARTAN 04 programme and was docked into the cyclodextrin cavity using iMol.

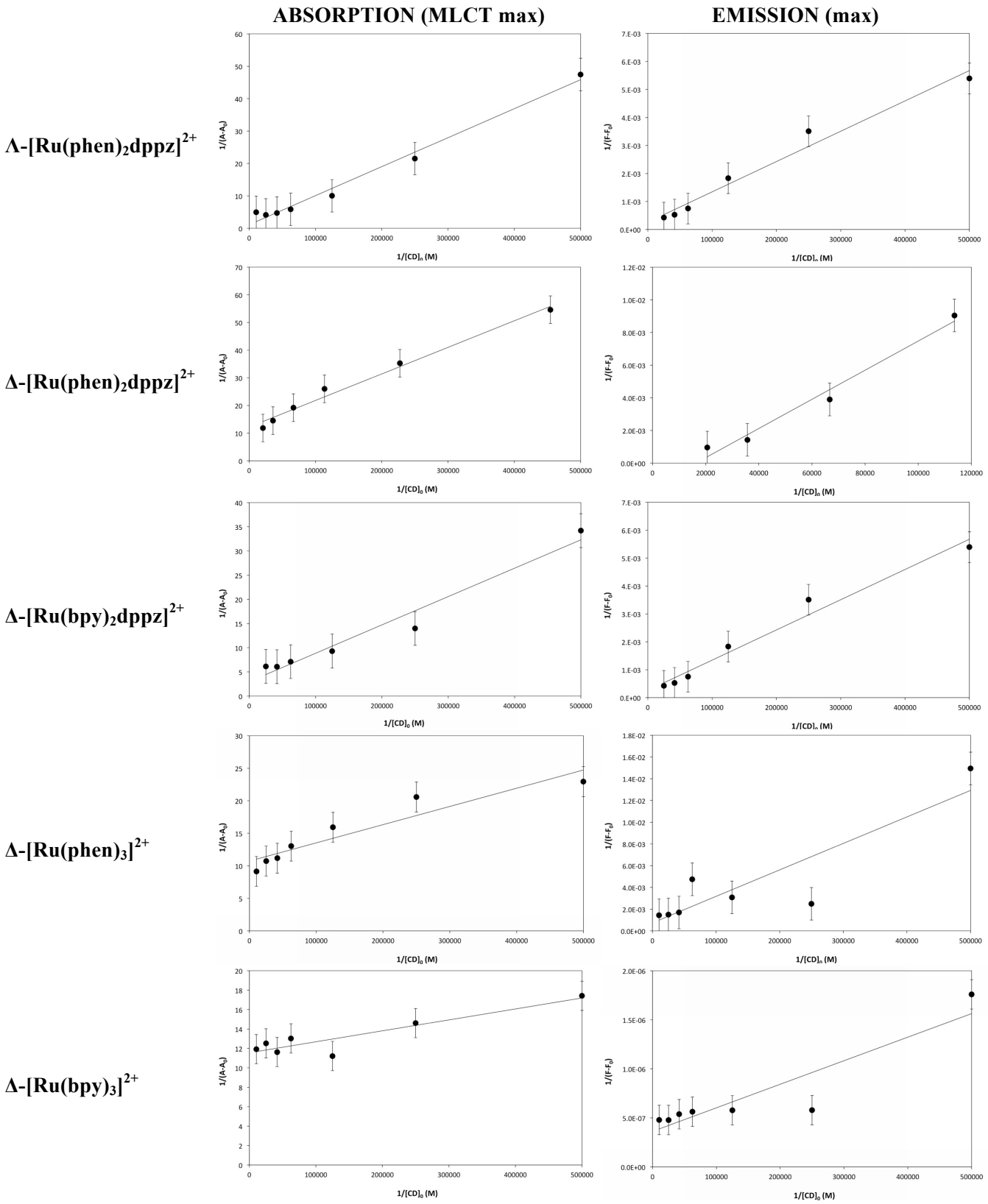

Figure S25. Benesi-Hildebrand binding plots at low binding ratios.